Direct Electrochemistry of Uric Acid at Chemically Assembled Carboxylated Single-Walled Carbon Nanotubes Netlike Electrode

Xing-Jiu Huang,*,† Hyung-Soon Im,† Oktay Yarimaga,† Ju-Hyun Kim,† Do-Hoon Lee,‡ Hak-Sung Kim,‡ and Yang-Kyu Choi†

Nano-Bio-Electronic Lab, Department of Electrical Engineering and Computer Science and Department of Biological Sciences, Korea Advanced Institute of Science and Technology, 373-1 Guseong-dong, Yuseong-gu, Daejeon, South Korea

Received: June 15, 2006; In Final Form: August 6, 2006

Carboxylated single-walled carbon nanotubes (SWCNT) chemically assembled on gold substrate was employed as netlike electrode to investigate the charge-transfer process and electrode process kinetics using uric acid as an example. The electrochemical behavior of uric acid in carboxylated SWCNT system was investigated using cyclic voltammetry, chronoamperometry, and single potential time-based techniques. The properties of raw SWCNT electrode were also studied for comparison purpose. Uric acid has better electrochemical behavior whereas ascorbic acid has no effective reaction on the carboxylated SWCNT electrode. Cyclic voltammograms indicate that the assembled carboxylated SWCNT increases more active sites on electrode surface and slows down the electron transfer between the gold electrode and uric acid in solution. The charge-transfer coefficient (α) for uric acid and the rate constant (k) for the catalytic reaction were calculated as 0.52 and 0.43 s^{-1}, respectively. The diffusion coefficient of 0.5 mM uric acid was 7.5×10^{-6} $cm^2 \cdot s^{-1}$. The results indicate that electrode process in the carboxylated SWCNT electrode system is governed by the surface adsorption-controlled electrochemical process.

1. Introduction

Uric acid is a very important biomolecule owing to its abnormal levels, which are the symptoms of several diseases such as gout, hyperuricaemia, and Lesch-Nyhan syndrome. Various methods have been reported for its determination, such as chemiluminescence,[1] chromatogram,[2] spectrofluorometric,[3] enzymatic system,[4] and so forth. The electrochemical techniques for detection of uric acid and ascorbic acid (main interferent) have received considerable interest in recent years because of their higher selectivity and rapid detection. Most of the attention has been focused on electrode surface modification by utilizing the materials including carbon materials,[5] biomolecule materials,[6] polymers,[7] organic matters,[8] and others.[9] Single-walled carbon nanotube (SWCNT) has recently been used in nanodevices and sensors[10] because of its unique structural, mechanical, and electronic properties.[11] Layer-by-layer assembly technique is an approach based on the alternating adsorption of materials containing complementary charged or functional groups to form integrated ultrathin films.[12] This method provides a powerful tool for nano- and microscale assembly of devices and novel material systems.[13] However, few reports are available on chemically assembled netlike carboxylated SWCNT for investigating the charge-transfer process and electrode process kinetics using uric acid as an example. Recently, Wei et al.[5c] reported that they prepared an SWCNT-modified gold electrode via physical adsorption for uric acid analysis. On the basis of our previous reports,[14,15] we prepare a carboxylated SWCNT netlike electrode using chemical assembly techniques for uric acid determination and investigate the charge-transfer process and electrode process kinetics in SWCNT electrode system. We found that the electrochemical behavior was different from that in SWCNT electrode system prepared using physical adsorption. The electrochemical behavior of uric acid was investigated by cyclic voltammetry, chronoamperometry, and single potential time-based techniques. The charge-transfer coefficient (α) for uric acid, the rate constant (k) for the catalytic reaction, and the diffusion coefficient of uric acid were calculated to analyze the electrode process.

2. Experimental Section

Reagents. Uric acid, ascorbic acid, and 11-amino-1-undecanethiol, hydrochloride were purchased from Sigma-Aldrich. The 11-amino-1-undecanethiol, hydrochloride solution was prepared by dissolving it in ethanol, and concentration was adjusted to 2 mM. SWCNT (1−10 nm in diameter, 5−20 μm in length) was obtained from Iljin Nanotech Co.,Ltd. (Korea). Other reagents were commercially available and were of analytical grade. Double deionized water (DDW) was used in all measurements. A phosphate-buffered saline solution (PBS, pH 7.4) was prepared by dissolving 1.6 g KCl, 64 g NaCl, 1.92 g KH_2PO_4, and 11.52 g K_2HPO_4 in 800 mL of DDW. Au and Ag/AgCl (saturated KCl solution) electrodes were purchased from CH Instruments, Inc. (United States) and Pt wire electrode was obtained from Bioelectrical System, Inc. (United States).

SAM (Self-Assembly Monolayer) Formation. Prior to assembling, the Au electrode was cleaned electrochemically by cycling it in 0.05 M H_2SO_4 solution between −500 mV and +1200 mV (versus Ag/AgCl) with a scan rate of 150 $mV \cdot s^{-1}$ until a reproducible cyclic voltammogram was achieved (typically 40 cycles) and then was rinsed thoroughly with DDW and was dried in a stream of high-purity N_2. 11-Amino-1-unde-

* Author to whom correspondence should be addressed. Tel: 82-42-869-8077. E-mail: xingjiuhuang@hotmail.com.

† Department of Electrical Engineering and Computer Science, Korea Advanced Institute of Science and Technology.

‡ Department of Biological Sciences, Korea Advanced Institute of Science and Technology.

10.1021/jp063749q CCC: $33.50
Published on Web 10/10/2006

canethiol, hydrochloride solution was dropped onto the active area of the Au electrode five times, followed by exhaustive washing using ethanol and DDW 6 h later and then was dried at room temperature. Typically a 20-μL aliquot of 11-amino-1-undecanethiol, hydrochloride solution would form the needed monolayer on Au surface.

Preparation of Carboxylated SWCNT Netlike Electrode. Two milligrams raw SWCNT was chemically shortened by oxidation in a 10-mL mixture of concentrated sulfuric and nitric acids (3:1, 98% and 70%, respectively[16]), and this mixture was subjected to sonication for 8 h at 40 °C in the water bath. This procedure introduces carboxylic acid functionalities and defects at the ends of the nanotubes as well as some carboxylic acid units at the sidewalls.[17] The shortened SWCNT was then collected first by filtering using 0.1-μm nitrocellulose membranes (Advantec MFS, Inc. Dublin, CA) and was washed until neutral pH was achieved before dispersing in 10 mL of ethanol. The ethanol was selected as solvent here because the filter membrane can be dissolved in acetone. After ethanol volatilizing completely, the shortened SWCNT was redispersed in acetone and, hence, we found the as-studied pipes can be well-solubilized by using a short 30-min sonication. The SWCNT netlike structure on Au surface was formed by depositing droplets of shortened SWCNTs dispersed in acetone onto an 11-amino-1-undecanethiol, hydrochloride modified gold surface. First, SWCNTs were assembled on the Au surface easily because of the condensation reaction between the $-$COOH and $-NH_2$ to form an interdigitated thin layer which is different from multilayer in the thickness. This step is different from physical adsorption, as evidenced by the stability of the layers when ultrasonicated. Then, with increasing SWCNT concentration or deposition cycles, many SWCNTs were sequentially adsorbed onto the Au surface to form interdigitated multilayer because of electrostatic and van der Waals interactions. In the experiment, deposition cycle is defined as the process performed from dropping the first SWCNT solution to the second one. The raw SWCNT electrode was also prepared by using original SWCNT (i.e., without mixture acid pretreating) for comparison purpose.

Scanning Electron Microscope (SEM) and Electrochemical Measurements. All of the SEM images were obtained with Philips XL 30 AFEG scanning electron microscope (Eindhoven, The Netherlands). Cyclic voltammetry (CV) measurements were performed on a BAS 100W electrochemical analyzer (Bioanalytical Systems, Inc., United States). All CV experiments were carried out in PBS solution in a conventional three-electrode cell at room temperature. Ag/AgCl and Pt wire were employed as reference and counter electrode, respectively.

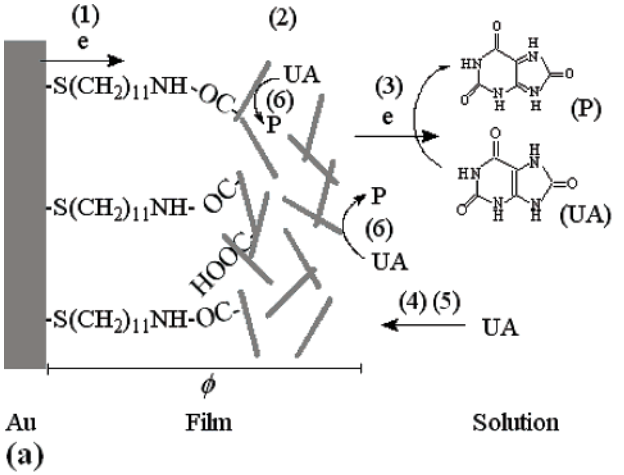

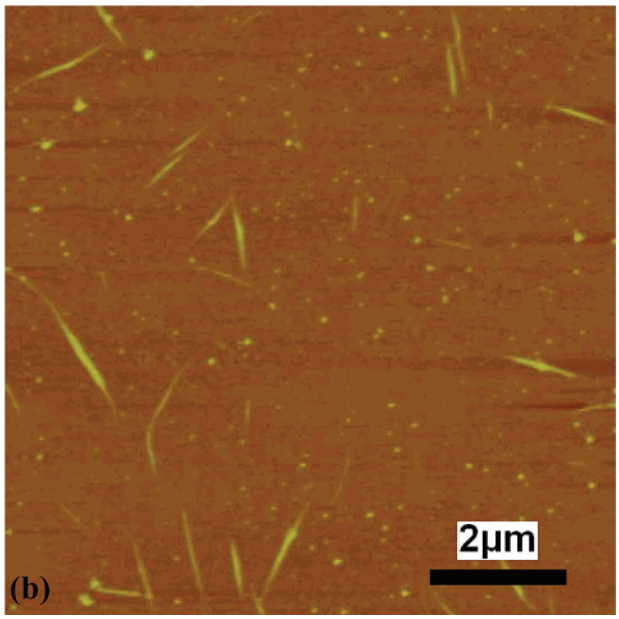

Figure 1. (a) The assembly of the carboxylated SWCNT netlike system on a Au electrode and processes and charge transport in the system. (1) Heterogeneous electron transfer to SWCNTs; (2) electron transfers within SWCNT; (3) electron transfers from SWCNT to uric acid; (4) penetration of uric acid into the film; (5) movement of uric acid through a pinhole or channel in the film to the Au substrate, where it can be oxidized; (6) electron transfers from defect sites in tube sides and ends to uric acid. (b) Typical AFM image of shortened SWCNTs (after sonication for 8 h at 40 °C); some are aggregates of several tubes in van der Waals contact.

3. Results and Discussion

Morphological Characterization. Figure 1a depicts the method to assemble the carboxylated SWCNT multilayer on a Au electrode and the diagram of processes that can occur at the modified electrode. The netlike SWCNT is based on films thicker than the monolayers, therefore, the typical charge transfer can be considered to include the following steps: (1) heterogeneous electron transfer to SWCNTs; (2) electron transfers within SWCNT; (3) electron transfers from SWCNT to uric acid; (4) penetration of uric acid into the film; (5) movement of uric acid through a pinhole or channel in the film to the Au substrate, where it can be oxidized; and (6) electron transfers from defect sites in tube sides and ends to uric acid. The raw SWCNTs were purified and cut by using a mixture of concentrated sulfuric and nitric acids to yield CNTs with an average length of about 0.5$-$1.5 μm. Typical atomic force microscopy (AFM) image (Figure 1b) indicates that the morphology of the SWCNT bundles changed from that of highly entangled strands (Figure 2d) to flexible rodlike ones which were thoroughly dispersed in acetone and existed in shortened tube bundles after etching. Taking AFM tip broadening into account, some of those apparent individual tubes are actually the aggregates of several tubes in van der Waals contact.[16] The FT-IR spectrum (data not shown) strongly suggests that the carbon nanotubes are terminated with carboxylic acid groups ($-$COOH, IR stretching vibration frequency $\upsilon_{C=O} = 1638$ cm^{-1}) and carboxylate groups ($-COO^-$, $\upsilon_{C=O} = 1530$ cm^{-1}) after oxidation treatment.

Figure 2a and 2b presents that carboxylated SWCNTs were assembled on the gold surface by controlling the deposition cycles of SWCNT. It is found that SWCNTs were chemisorbed onto the gold surface to form uniform an interdigitated multilayer via Au$-$S covalent bond, $-$NH$-$CO$-$ covalent bond, and

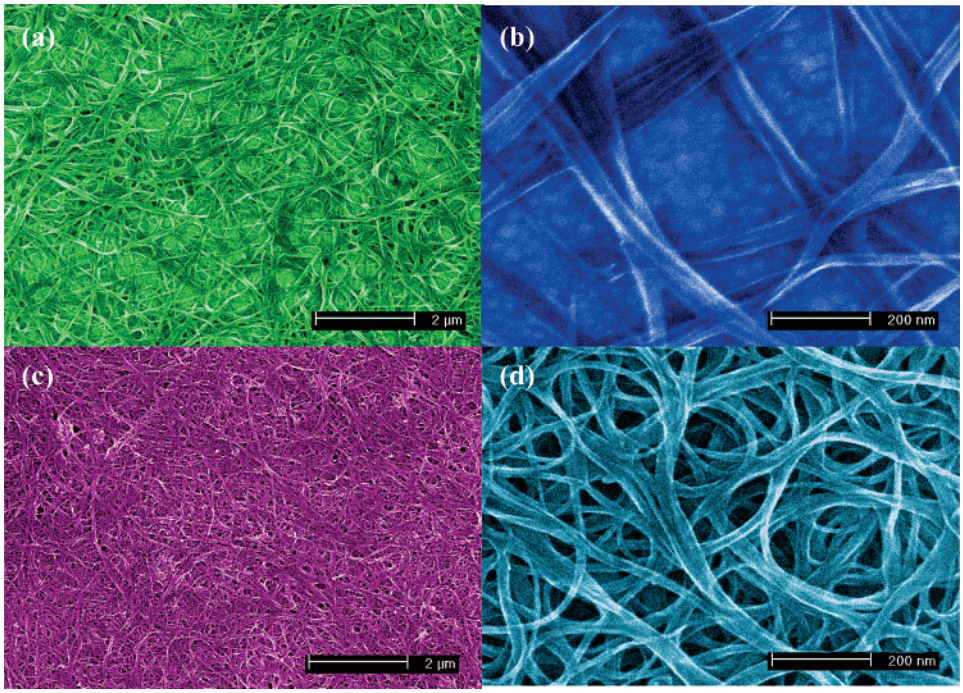

Figure 2. Typical SEM images of SWCNT electrode surface with different magnification at the given concentration of 2 mg·L^{-1} (a, c: 10 000×, b, d: 100 000×). Images a and b corresponding to carboxylated SWCNT after cutting by an acid mixture; images c and d show the raw SWCNT before cutting. Ten deposition cycles for images a and b; two cycles for images c and d.

electrostatic and van der Waals interactions between the carbon nanotubes. Figure 2c and 2d shows the surface properties of raw SWCNT modified gold electrode via physical adsorption. In the figure, raw SWCNT can also form a netlike structure on gold surface. Then, there rises an important question: How about their electrochemical behavior in uric acid that they can all form net structure on gold surface? The experimental results demonstrate that the electrochemical behavior of carboxylated SWCNT net electrode is much better that that of raw SWCNT electrode, as will be considered in more detail in the following section.

Cyclic Voltammogram Behavior of Uric Acid. Figure 3 indicates the comparison of bare gold, 11-amino-1-undecanethiol monolayer assembled Au electrode, raw SWCNT, and carboxylated SWCNT netlike electrode in uric acid/PBS solution at scan rate of 100 mV·s^{-1}. First, no current peak for uric acid can be observed at bare gold electrode, suggesting that it is hard for uric acid to accumulate at gold electrode surface or that the electrochemical reaction is very slow. However, after assembling 11-amino-1-undecanethiol monolayer, electron transfer between metal substrate and analyte in solution is almost totally hindered by the monolayer, which is in agreement with the previous report.[17b] Subsequently, the electrochemical behavior of chemically assembled SWCNT electrode can be explained by considering electrode electron tunneling process across the monolayer.[17b] Second, at the raw SWCNT electrode, we can observe a residual current (Figure 3b) which is composed of a current because of double-layer charging and a current caused by low-level oxidation of components in the system. This is explained by considering that the raw SWCNT contains trace impurities such as heavy metals and the raw SWCNT electrode undergoes slow and potential-dependent Faradaic reactions.[18] Finally, at the carboxylated SWCNT electrode, a sensitive anodic peak occurs at about 370 mV. It can be inferred that uric acid can effectively accumulate at the carboxylated SWCNT surface and its electrochemical oxidation was promoted. This is because the as-studied carboxylated SWCNT electrode has a highly permeable "net" structure. On the other hand, the acid

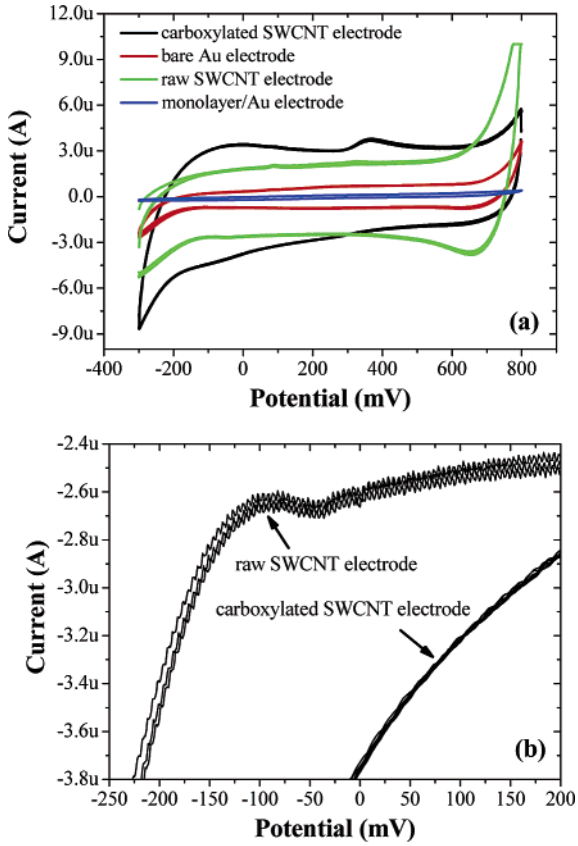

Figure 3. (a) Potential window of bare gold, 11-amino-1-undecanethiol monolayer assembled Au electrode, raw SWCNT, and carboxylated SWCNT electrode in 5 μM uric acid/PBS solution at scan rate of 100 mV·s^{-1}; (b) residual current curve for 5 μM uric acid at raw SWCNT electrode.

treatment creates more oxide defects on the tube sidewalls and ends which can be involved in the redox reaction and makes the SWCNT more hydrophilic so that the sample can contact

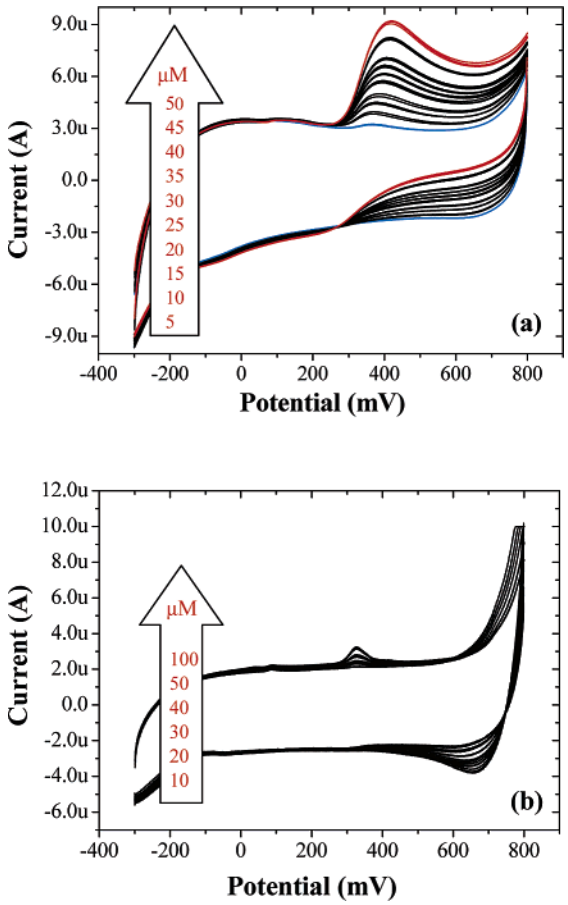

Figure 4. Cyclic voltammograms of uric acid/PBS under different concentrations obtained with carboxylated SWCNT electrode (a) and raw SWCNT electrode (b). Scan rate of 100 mV·s^{-1}, pH 7.4.

the surface better.[19] Also, the voltammetric peak at the carboxylated SWCNT electrode is broad, suggesting slow electron transfer kinetics, presumably because of the macroscopical planelike structure. At the same time, the current separation between the forward and backward scans becomes greater than that of raw SWCNT. This agrees with the large capacitance feature reported before,[20] that is, the capacitance is calculated from the cyclic voltammogram curves, with $C = i/\upsilon$, where i is the current and υ is the scan rate (V/s). At the potential of −0.03 V, for example, the effective capacitance is about 1 time larger than that of raw SWCNT and over 10 times larger than that of the bare gold electrode. This high capacitance is consistent with the large surface area of the net carboxylated SWCNT.[20a]

We further measured the cyclic voltammograms of uric acid/PBS under different concentrations at scan rate of 100 mV·s^{-1} obtained with carboxylated SWCNT electrode, as shown in Figure 4a. Obviously, the anodic current (i_{pa}) increases gradually with increasing concentration of uric acid while the anodic peak potential shows a positive shift from 365 mV to 425 mV. Similar behavior can be observed under different scan rates. In comparison, at the raw SWCNT electrode, no obvious anodic current or cathodic current peak can be observed even for the increment of concentration up to 0.1 mM (Figure 4b) demonstrating that no obvious electrochemical reaction occurs in the raw SWCNT electrode system. This suggests that the electrochemical activity of carboxylated SWCNT is better than that of raw SWCNT even though both have net structure. As seen from Figure 4a, we cannot observe any cathodic peak which means that uric acid can be irreversibly electrochemically oxidized in aqueous solution. The proposed reaction mechanism

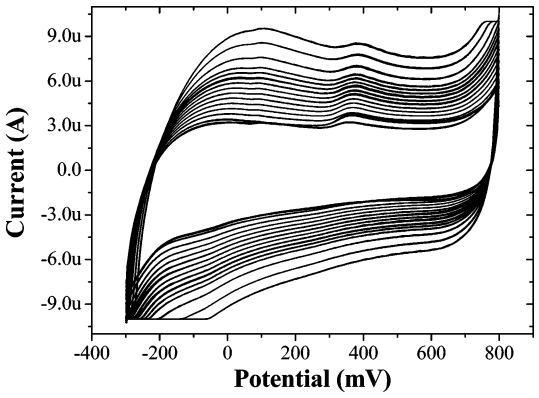

Figure 5. Cyclic voltammograms of carboxylated SWCNT electrode in 10 μM uric acid at different scan rates, from inside to outside: 90, 100, 110, 120, 130, 140, 150, 160, 170, 180, 190, 200, 220, 250, and 280 mV·s^{-1}, respectively.

SCHEME 1: Electrochemical Oxidation Reaction of Uric Acid

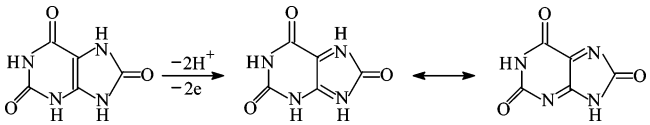

is shown in Scheme 1 by considering the earlier studies.[15c]

Figure 5 shows the cyclic voltammograms of the carboxylated SWCNT electrode in uric acid/PBS at various scan rates. It is found that the anodic peak potential shifts positively from 360 mV to 388 mV for different scan rates. This is most probably due to the electrocatalytic and kinetic effect of carboxylated SWCNT netlike surface on the oxidation uric acid. The carboxylated SWCNT increases more active sites on electrode surface and slows down the electron transfer from the gold to uric acid in solution. Fitting the peak height for the anodic potential (data not shown), E_{pa} was found to be a linear function of log υ at scan rates from 90 to 280 mV·s^{-1}, which the linear regression equation is $E_{pa} = 252.7 + 56.8 \log \upsilon$ (E_{pa}: mV, υ: mV·s^{-1}, $r = 0.995$). The electron-transfer coefficient α can be easily calculated to be 0.52 by using Laviron's equations:[21]

$$E_{pa} = E^j + \frac{RT}{(1-\alpha)nF}\ln\left[\frac{1-\alpha}{m}\right] = E^j + \frac{RT}{(1-\alpha)nF}\ln\left[\frac{(1-\alpha)n\upsilon F}{RTk_s}\right]$$

$$= E^j + \frac{2.303RT}{(1-\alpha)nF}\log\left[\frac{(1-\alpha)nF}{RTk_s}\right] + \frac{2.303RT}{(1-\alpha)nF}\log \upsilon$$

n, F, υ, R, and T have their usual significance. k_s can be calculated with the help of the following equation as 0.43 s^{-1} which is in agreement with the range of values of most previous reports.[21b,22]

$$\log k_s = \alpha\log(1-\alpha) + (1-\alpha)\log\alpha - \log\frac{RT}{nF\upsilon} - \frac{\alpha(1-\alpha)nF\Delta E_p}{2.303RT}$$

By considering the cyclic voltammogram behavior of uric acid, we know that there is an anodic peak at about 365 mV, so the anodic current (i_{pa}) at potential of 365 mV is selected to represent the baselines plotted versus the scan rate (υ) in Figure 6a. Clearly, it is linearly proportional to the scan rate, and the regression equation is $i_{pa} = 0.702 + 0.029\upsilon$, $r = 0.998$ (i_{pa}:

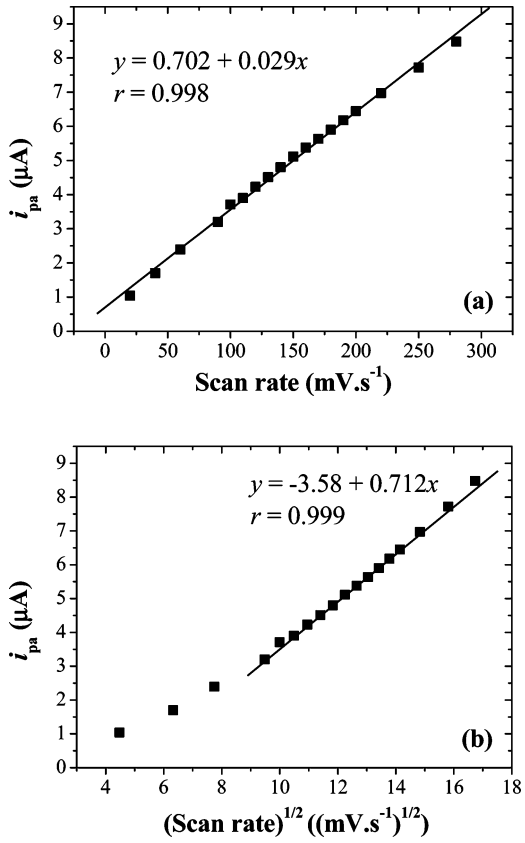

Figure 6. (a) Anodic current (i_{pa}) of the cyclic voltammograms at 365 mV obtained with carboxylated SWCNT electrode vs the scan rate; (b) anodic peak height vs the square root of the scan rate.

μA, v: mV·s^{-1}), indicating that the adsorbed uric acid on carboxylated SWCNT shows a reversible and surface-confined electrochemical process. We also fit the peak heights for the anodic currents (i_{pa}), as shown in Figure 6b. The i_{pa} is found to be a linear function of the square root of the scan rate from 90 to 280 mV·S^{-1}, which is similar to a solid macroelectrode rather than nanoelectrode ensembles. This is likely because the carboxylated SWCNT netlike electrode has a very high packing density with average pore size of hundreds of nm, which is much smaller than the diffusion layer thickness ($j_{max} \sim (Dt)^{1/2}$, D: diffusion coefficient, t: time, normally over micrometers).[23] The diffusion layers originating at individual nanotube or bundles are heavily overlapped. Accordingly, the voltammetric response to uric acid will no longer resemble that of individual microelectrodes but rather will display characteristics similar to a macroelectrode cyclic voltammetry.[24] Therefore, we suggest that electrode process in the carboxylated SWCNT netlike electrode system is determined by the surface adsorption-controlled electrochemical process.

Real-Time Behavior of Uric Acid. Figure 7 shows the measurement of current as a function of time and solution concentration at carboxylated SWCNT net electrode. It is obvious that the current increases stepwise with discrete changes in concentration of uric acid from 2.5 to 17.5 μM and that the current is constant for a given concentration. The response is very fast in reaching a dynamic equilibrium upon each addition of the sample solution, and a steady-state current signal was generated within several seconds. The changes in current are also reversible for increasing or decreasing uric acid concentration. A typical plot of the peak current versus concentration (the inset in Figure 7) shows that this concentration dependence is linear between the range of 2.5 and 17.5 μM. The chrono-

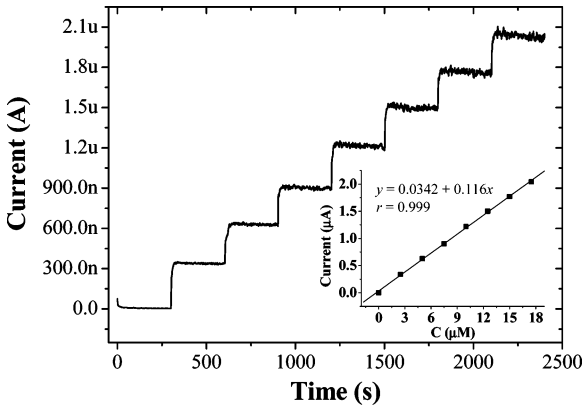

Figure 7. Real-time detection of the current for carboxylated SWCNT net electrode in uric acid solution for concentrations from 2.5 to 17.5 μM (each addition: 2.5 μM); the applied potential was 365 mV. The inset shows plot of the current versus concentration; the black square points are experimental data, and the line is linearly fit to these data.

amperometry was also employed for the inverstigation of electrode processes at chemically assembled SWCNT electrode. For an electroactive material with diffusion coefficient D, the current corresponding to the electrochemical reaction is described by Cottrell's equation[25]

$$I(t) = nFAC^*(D/\pi t)^{1/2}$$

where D and C^* are the diffusion coefficient (cm^2·s^{-1}) and the bulk concentration (mol·cm^{-3}), respectively. The diffusion coefficient is calculated from the slope of the plot of I versus $t^{-1/2}$ to give 7.5×10^{-6} cm^2·s^{-1} (0.5 mM uric acid) which agrees reasonably with other previous reports.[5e, 22b]

Cyclic Voltammogram Behavior of Uric Acid and Ascorbic Acid Mixture. In many previous reports, the oxidation peak of the mixture of uric acid and ascorbic acid was successfully separated at modified electrodes,[5−9] that is, the two acids can be oxidized at different potentials whereas the locations of oxidation potential for the mixture are the same as those for single uric acid or ascorbic acid. However, this is not the case for carboxylated SWCNT netlike electrode used in our study. Figure 8 shows the electrochemical behavior of uric acid and ascorbic acid in the mixture when the concentration of one species changed, whereas the other one is kept constant. First, no oxidation peak of ascorbic acid can be observed at carboxylated SWCNT electrode. This indicates that ascorbic acid cannot effectively accumulate at SWCNT surface and has no electrochemical activity, even though increasing its concentration. Second, neither of the two oxidation peaks can be observed for uric acid and ascorbic acid mixture at carboxylated SWCNT electrode. This case is very different from the previous findings of Wei et al.[5c] which can be explained by considering that the chemical and electrochemical properties of the SWCNT are strongly dependent on the postgrowth processing procedures and acid treatment procedures.[24] In Figure 8a, adding the ascorbic acid to 40 μM uric acid in discrete mode, we only find one anodic peak which is the same as that for single uric acid. For confirmation, we studied the case through trial-and-error method, and we observed that there is still one anodic peak. Meanwhile, the cyclic voltammograms of the mixture are similar to those of single uric acid at different concentrations. In Figure 8b, keeping the ascorbic acid concentration constant, the anodic peak current appears even with the addition of trace uric acid such as 5 μM. Moreover, the electrochemical behavior is similar to that of single uric acid. The exact mechanism is not clear at present, but we believe that adding ascorbic acid

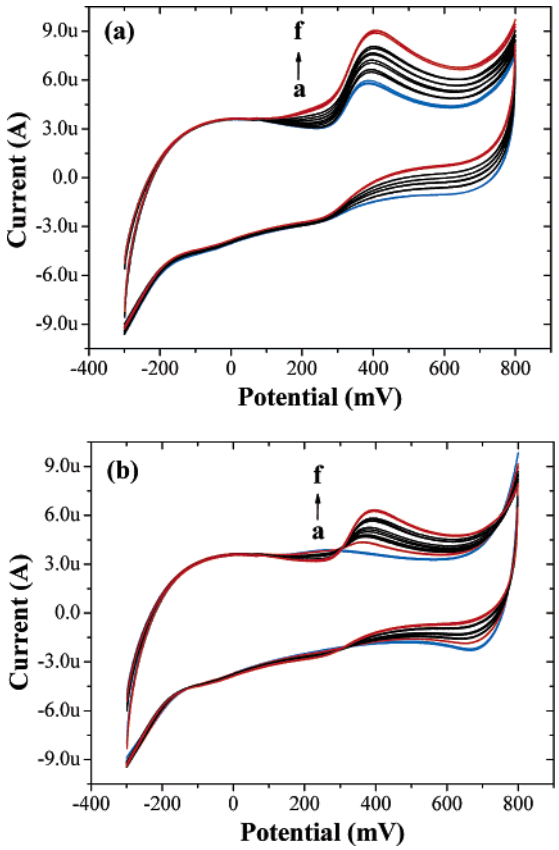

Figure 8. Cyclic voltammograms for the mixture of uric acid and ascorbic acid with different concentrations in PBS buffer at the carboxylated SWCNT electrode. (a) Uric acid (40 μM) and ascorbic acid (a−f: 0, 50, 100, 150, 200, 250 μM); (b) ascorbic acid (40 μM) and uric acid (a−f: 0, 5, 10, 15, 20, 25 μM).

may make uric acid accumulate on carboxylated SWCNT electrode surface. Future studies will be required to resolve the contribution. We therefore suggest that the carboxylated SWCNT electrode has a perfect electrochemical activity with uric acid whereas ascorbic acid has no obvious effect on the determination of uric acid.

4. Conclusion

A carboxylated SWCNT netlike electrode was prepared by combining layer-by-layer assembly technique and the reaction of carboxylic SWCNT with amino group. Electrochemical behavior of uric acid at carboxylated SWCNT netlike electrode and its selective determination in the presence of ascorbic acid were investigated. Carboxylated SWCNT electrode exhibits stronger electrochemical activity to uric acid than that of bare gold and raw SWCNT electrode. The charge-transfer coefficient (α) for uric acid was calculated as 0.52. The rate constant (k) for the catalytic reaction was also determined to be 0.43 s^{-1}. The diffusion coefficient of 0.5 mM uric acid was 7.5×10^{-6} $cm^2 \cdot s^{-1}$. The results indicate that electrode process in the as-studied SWCNT electrode system is determined by the surface adsorption-controlled electrochemical process. Carboxylated SWCNT electrode shows a stable and reproducible response to uric acid, whereas ascorbic acid has no effective electrochemical reaction on the electrode surface. The lowest concentration of uric acid reaches 2.5 μM. A good linear relationship between current and concentration was obtained for the range from 2.5 to 17.5 μM. Future works will be focused on exploring why ascorbic acid makes uric acid accumulate on carboxylated SWCNT electrode surface and the effect of the thickness of SWCNT on sensitivity.

Acknowledgment. This work was supported by Brain Korea 21 project, the School of Information Technology, Korea Advanced Institute of Science and Technology in 2006, and the National Research and Development Program (NRDP, 2005-01274) for the biomedical function monitoring biosensor development sponsored by the Korea Ministry of Science and Technology (MOST).

References and Notes

(1) (a) Han, S. Q.; Liu, E. B.; Li, H. *Anal. Sci.* **2005**, *21*, 111−114. (b) He, D. Y.; Zhang, Z. J.; Huang, Y.; Hu, Y. F.; Zhou, H. J.; Chen, D. L. *Luminescence* **2005**, *20*, 271−275. (c) Lv, Y.; Zhang, Z. J.; Chen, F. N. *Analyst* **2002**, *127*, 1176−1179. (d) Liu, E. B.; Wei, H. Q. *Spectrosc. Spectrosc. Anal.* **2005**, *25*, 1213−1215.

(2) (a) Perelló, J.; Sanchis, P.; Grases, F. *J. Chromatogr., B* **2005**, *824*, 175−180. (b) Inoue, K.; Namiki, T.; Iwasaki, Y.; Yoshimura, Y.; Nakazawa, H. *J. Chromatogr., B* **2003**, *785*, 57−63.

(3) (a) Martinez-Pérez, D.; Ferrer, M. L.; Reyes Mateo, C. *Anal. Biochem.* **2003**, *322*, 238−242. (b) Oda, J.; Shinmoto, E.; Shiozaki, A.; Hatae, Y.; Katayama, S.; Jiao, G. S. *J. Health Sci.* **2004**, *50*, 594−599.

(4) (a) Akyilmaz, E.; Kemal Sezgintürk, M.; Dinçkaya, E. *Talanta* **2003**, *61*, 73−79. (b) Jelikić-Stankov, M.; Djurdjević, P.; Stankov, D. *J. Serb. Chem. Soc.* **2003**, *68*, 691−698.

(5) (a) Ye, J. S.; Wen, Y.; Zhang, W. D.; Gan, L. M.; Xu, G. Q.; Sheu, F. S. *Electroanalysis* **2003**, *15*, 1693−1698. (b) Ramesh, P.; Sampath, S. *Electroanalysis* **2004**, *16*, 866−869. (c) Wei, S. H.; Zhao, F. Q.; Zeng, B. Z. *Microchim. Acta* **2005**, *150*, 219−224. (d) Goyal, R. N.; Gupta, V. K.; Sangal, A.; Bachheti, N. *Electroanalysis* **2005**, *17*, 2217−2223. (e) Ardakani, M. M.; Akrami, Z.; Kazemian, H.; Zare, H. R. *J. Electroanal. Chem.* **2006**, *586*, 31−38.

(6) (a) Zhang, L.; Lin, X. Q. *Analyst* **2001**, *126*, 367−370. (b) Wang, S. Q.; Lu, L. P.; Lin, X. Q. *Electroanalysis* **2004**, *16*, 1734−1738. (c) Lu, L. P.; Lin, X. Q. *Anal. Sci.* **2004**, *20*, 527−530. (d) Luo, J. W.; Zhang, M.; Pang, D. W. *Sens. Actuators, B* **2005**, *106*, 358−362. (e) Zare, H. R.; Memarzadeh, F.; Ardakani, M. M.; Namazian, M.; Golabi, S. M. *Electrochim. Acta* **2005**, *50*, 3495−3502. (f) Lin, X. Q.; Jin, G. P. *Electrochim. Acta* **2005**, *50*, 3210−3216. (g) Ren, W.; Luo, H. Q.; Li, N. B. *Biosens. Bioelectron.* **2006**, *21*, 1086−1092.

(7) (a) Fei, J. J.; Wu, K. B.; Wu, Y. H.; Hu, S. S. *J. Solid State Eletrochem.* **2004**, *8*, 316−321. (b) Roy, P. R.; Okajima, T.; Ohsaka, T. *J. Electroanal. Chem.* **2004**, 561, 75−82. (c) Kumar, S. S.; Mathiyarasu, J.; Phani, K. L.; Jain, Y. K.; Yegnaraman, V. *Electroanalysis* **2005**, 17, 2281−2286. (d) Kalimuthu, P.; Abraham John, S. *Electrochem. Commun.* **2005**, *7*, 1271−1276. (e) Li, N. B.; Niu, L. M.; Luo, H. Q. *Microchim. Acta* **2006**, *153*, 37−44.

(8) (a) Zheng, L. Z.; Wu, S. G.; Lin, X. Q.; Nie, L.; Rui, L. *Electroanalysis* **2001**, *13*, 1351−1354. (b) Khoo, S. B.; Chen, F. *Anal. Chem.* **2002**, *74*, 5734−5741. (c) Raj, C. R.; Ohsaka, T. *J.* Electroanal. Chem. **2003**, *540*, 69−77. (d) Liu, C. Y.; Lu, G. H.; Jiang, L. Y.; Jiang, L. P.; Zhou, X. C. *Electroanalysis* **2006**, *18*, 291−297.

(9) (a) Shi, K.; Shiu, K. K. *Electroanalysis* **2001**, *13*, 1319−1325. (b) Sun, Y. Y.; Fei, J. J.; Wu, K. B.; Hu, S. S. *Anal. Bioanal. Chem.* **2003**, *375*, 544−549. (c) Premkumar, J.; Khoo, S. B. *J. Electroanal. Chem.* **2005**, *576*, 105−112.

(10) (a) Santhanam, K. S. V.; Sangoi, R.; Fuller, L. *Sens. Actuators, B* **2005**, *106*, 766−771. (b) Barone, P. W.; Baik, S.; Heller, D. A.; Strano, M. S. *Nat. Mater.* **2005**, *4*, 86−92.

(11) Xiao, Y.; Patolsky, F.; Katz, E.; Hainfeld, J. F.; Willner, I. *Science* **2003**, *299*, 1877−1881.

(12) Mamedov, A.; Ostrander, J.; Aliev, F.; Kotov, N. A. *Langmuir* **2000**, *16*, 3941−3949.

(13) Bruening, M. L.; Sullivan, D. M. *Chem.—Eur. J.* **2002**, *8*, 3833−3837.

(14) (a) Lee, D; Lee, J.; Kim, J.; Kim, J.; Na, H. B.; Kim, B.; Shin C. H.; Kwak, J. H.; Dohnalkova, A.; Grate, J. W.; Hyeon, T.; Kim, H. S. *Adv. Mater.* **2005**, *17*, 2828−2833. (b) Lee, J.; Lee, D.; Oh, E.; Kim. J.; Kim, Y. P.; Jin, S.; Kim, H. S.; Hwang, Y.; Kwak, J. H.; Park, J. G.; Shin C. H.; Kim, J.; Hyeon, T. *Angew. Chem., Int. Ed.* **2005**, *44*, 7427−7432.

(15) Huang, X. J.; Li, Y.; Im, H. S. ; Yarimaga, O.; Kim, J. H.; Jang, D. Y.; Cho, S. O.; Cai, W. P.; Choi, Y. K. *Nanotechnology* **2006**, *17*, 2988−2993.

(16) Liu, J.; Rinzler, A. G.; Dai, H. J.; Hafner, J. H.; Bradley, R. K.; Boul, P. J.; Lu, A.; Iverson, T.; Shelimov, K.; Huffman, C. B.; Rodriguez-Macias, F.; Shon, Y. S.; Lee, T. R.; Colbert, D. T.; Smalley, R. E. *Science* **1998**, *280*, 1253−1256.

(17) (a) Wu, B.; Zhang, J.; Wei, Z.; Cai, S. M.; Liu, Z. F. *J. Phys. Chem. B* **2001**, *105*, 5075−5078. (b) Diao, P.; Liu, Z. F. *J. Phys. Chem. B* **2005**, *109*, 20906−20913. (c) Sheeney-Haj-Khia, L.; Basnar, B.; Willner, I. *Angew. Chem., Int. Ed.* **2005**, *44*, 78−83.

(18) Bard, A. J.; Faulkner, L. R. *Electrochemical Methods*; John Wiley & Sons: New York, 2001; pp 270−272.

(19) (a) Banks, C. E.; Davies, T. J.; Wildgoose, G. G.; Compton, R. G. *Chem. Commun.* **2005**, *7*, 829−841. (b) Banks, C. E.; Moore, R. R.; Davies, T. J.; Compton, R. G. *Chem. Commun.* **2004**, *16*, 1804−1805. (c) Chou, A.; Böcking, T.; Singh, N. K.; Gooding, J. J. *Chem. Commun.* **2005**, *7*, 842−844.

(20) (a) Liu, C. Y.; Bard, A. J.; Wudl, F.; Weitz, I.; Heath, J. R. *Electrochem. Solid−State Lett.* **1999**, *2*, 577−578. (b) Barisci, J. N.; Wallace, G. G.; Baughman, R. H. *J. Electrochem. Soc.* **2000**, *147*, 4580−4583.

(21) (a) Laviron, E. *J. Electroanal. Chem.* **1979**, *100*, 263−270. (b) Laviron, E. *J. Electroanal. Chem.* **1979**, *101*, 19−28.

(22) (a) Lötzbeyer, T.; Schuhmann, W.; Katz, E.; Falter, J.; Schmidt, H. L. *J. Electroanal. Chem.* 1994, *377*, 291−294. (b) Ernst, H.; Knoll, M. *Anal. Chim. Acta* **2001**, *449*, 129−134.

(23) Bard, A. J.; Faulkner, L. R. *Electrochemical Methods*; John Wiley & Sons: New York, 2001; pp 792−793.

(24) Li, J.; Cassell, A.; Delzeit, L.; Han, J.; Meyyappan, M. *J. Phys. Chem. B* **2002**, *106*, 9299−9305.

(25) Bard, A. J.; Faulkner, L. R. *Electrochemical Methods*; John Wiley & Sons: New York, 2001; pp 162−163.